ACS Photonics

Letter

pubs.acs.org/journal/apchd5

Hybrid Plasmonic Photonic Crystal Cavity for Enhancing Emission from near-Surface Nitrogen Vacancy Centers in Diamond

Shanying Cui,[†,⊥] Xingyu Zhang,[†] Tsung-li Liu,[†] Jonathan Lee,[†] David Bracher,[‡] Kenichi Ohno,[§] David Awschalom,[∥] and Evelyn L. Hu*[,†]

[†]School of Engineering and Applied Sciences, Harvard University, Cambridge, Massachusetts 02138, United States

[‡]Department of Physics, Harvard University, Cambridge, Massachusetts 02138, United States

[§]Department of Physics, University of California, Santa Barbara, California 93106, United States

[∥]Institute for Molecular Engineering, University of Chicago, Chicago, Illinois 60637, United States

Supporting Information

ABSTRACT: Optical cavities create regions of high field intensity, which can be used for selective spectral enhancement of emitters such as the nitrogen vacancy center (NV) in diamond. This report discusses a hybrid metal−diamond photonic crystal cavity, which provides greater localization of the electric field than dielectric cavities and mitigates metal-related losses in existing plasmonic structures. We fabricated such hybrid structures using silver and single-crystal diamond and observed emission enhancement of NVs near the diamond surface. We measured a mode quality factor (Q) as high as 170 with a simulated mode volume of ∼0.1 $(\lambda/n)^3$ and demonstrated its tunability. This cavity design and the associated fabrication approach specifically target enhancement of emission from near-surface NVs.

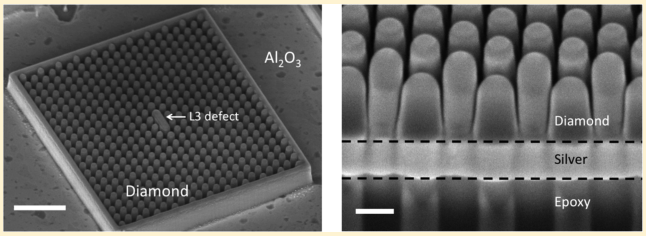

KEYWORDS: *plasmonics, photonic crystal, optical cavities, nitrogen vacancy centers*

Negatively charged nitrogen vacancy centers (NVs) in diamond have garnered much attention in recent years for their applications in nanoscale magnetometry[1,2] and potential for quantum information technologies.[3] For external magnetometry, NV centers should be placed as close as possible to the diamond surface, which serves as the interface with an external medium (thus we term these "near-surface" NV emitters). However, the poor collection of emission from bulk diamond and small branching ratio into the zero-phonon transition have prompted the use of optical waveguides and cavities to enhance NV emission and collection efficiency.[4] Recent progress in the fabrication of all-diamond optical cavities has produced measured quality factors $Q \approx 10^3$−10^4 and mode volumes $V \approx (\lambda/n)^3$.[5−7] However, despite these demonstrations of NV emission enhancement, there remain substantial challenges in both the strength of coupling of the cavity to the NV emission and, ultimately, the extraction of the emitted light from the cavity. In addition, such high-Q cavities have their field maxima located centrally within the diamond, away from the interfaces, and are therefore less effective in coupling to near-surface NVs.

Hybrid metal−dielectric cavities[8−10] combine the advantages of the highly localized optical fields characteristic of subwavelength plasmonic cavities with the precision fabrication achievable with dielectric materials, which allows control of the photonic band gap through periodic modulation of the dielectric material. Despite their relatively low quality factors ($Q \approx 100$), such hybrid cavities have better field confinement than dielectric cavities, with typical $V < 0.1$ $(\lambda/n)^3$, leading to Purcell enhancement comparable to all-diamond cavities. This report discusses the fabrication and performance of such a hybrid plasmonic photonic crystal cavity, implemented using diamond nanopillars and a silver substrate. We measured Q factors as high as 170 with simulated mode volumes ∼0.1 $(\lambda/n)^3$ at λ = 650 nm for a cavity geometry designed to couple regions of high field specifically to near-surface NVs to increase magnetometry sensitivities.

Our cavity geometry is based on the structure described in reference 11 and incorporates near-surface (∼10 nm from the diamond surface) NVs as the emitters. The fabricated cavity is composed of diamond nanopillars (n = 2.4) atop a silver substrate, with a 5 nm layer of Al_2O_3 (n = 1.8) sandwiched in between as the gap dielectric (Figure 1a). The diamond nanopillars are arranged in a hexagonal lattice, with center-to-center spacing, **a**. To create a cavity, the center of the lattice contains a linear defect, made up of three conjoined neighboring rods from the lattice, each with a radius of R, such that the length of the cavity is $L = 2(R + a)$. The cavity resonance can be tuned by altering various dimensions of the diamond photonic crystal and the defect size (e.g., through changing R). The cavity Q and vertical far-field radiation are

Received: December 13, 2014
Published: March 11, 2015

DOI: 10.1021/ph500469e
ACS Photonics 2015, 2, 465−469

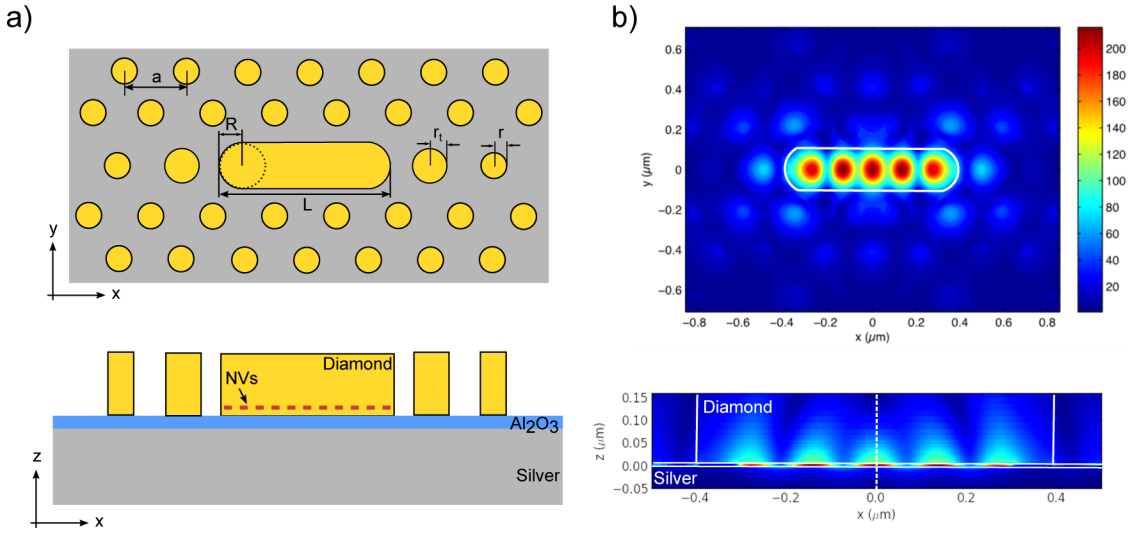

Figure 1. (a) Top-down and cross-sectional schematic of the hybrid plasmonic photonic crystal cavity and (b) simulated electric field profile of the cavity mode at 636 nm. The defect region is highlighted in white in the top-down view, and different materials are demarcated with white lines in the cross-sectional view.

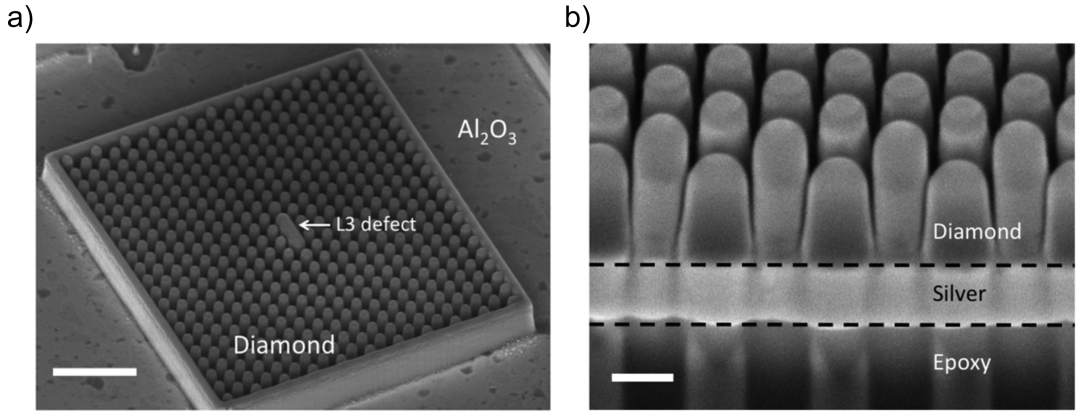

Figure 2. (a) Angled scanning electron micrograph at 45° vertical tilt of the diamond cavity (scale bar corresponds to 1 μm). (b) Focused ion beam cross-section of photonic crystal region (scale bar corresponds to 200 nm).

maximized by adjusting the radius r_t of the two rods neighboring the central defect. These design parameters provide flexibility in selecting the cavity resonance and improve the collection efficiency from the NVs in diamond.

RESULTS AND DISCUSSION

Finite-difference time-domain simulations (FDTD, Lumerical Solutions) are used to model the hybridized modes of the cavity. An electric dipole, representing shallow emitters, oriented perpendicular to the diamond dielectric interface was positioned 10 nm from the diamond−alumina interface. Diamond rods each with a radius r = 84 nm and a height = 400 nm are positioned in a hexagonal lattice with lattice constant a = 230 nm. R is varied between 1.2r and 1.3r to determine the dependence of the cavity mode resonance on the geometry. The electric field profile of the cavity mode, centered at 636 nm, is shown in Figure 1b. The electric field is highly confined within the lower-index alumina layer, but emitters near the diamond−alumina interface can evanescently couple to the defect mode with relatively high efficiency. We obtain a simulated Q value of ∼200, which is higher than previously proposed diamond plasmonic cavities.[10] The simulated effective mode volume of our fabricated structure is approximately 0.1 $(\lambda/n)^3$ for λ = 650 nm, leading to a Purcell factor of ∼30. While our Q value is higher than previously proposed diamond plasmonic cavities,[12] higher Q values and Purcell factors have been demonstrated and measured in all-dielectric devices.[5−7] Our device, however, is designed to more efficiently enhance near-surface NVs for magnetometry applications. Furthermore, both the presence of the silver mirror and the waveguide-like rods in the diamond significantly enhance the collection efficiency of the NV emission.

There are two main challenges for fabricating this structure (Figure 2). First, a diamond membrane a few hundred nanometers thick must be placed in direct contact with the thin Al_2O_3 layer. Single-crystal diamond cannot be grown onto an Al_2O_3 template. Moreover, it is impractical to first create the device from bulk diamond, then etch-remove hundreds of micrometers of diamond. Our solution involves beginning with a 200 × 200 μm size, 1 μm thick diamond membrane, which is bound to a silicon substrate with poly(methyl methacrylate) (PMMA).[7,13] NV ensembles ∼10 nm from the diamond surface are then created with ion implantation of ^{14}N (10 keV, 3×10^{13} ions/cm^2). Details of the diamond membrane fabrication and NV generation can be found in the Supporting Information. Using atomic layer deposition (ALD), we then deposit 5 nm of

DOI: 10.1021/ph500469e
ACS Photonics 2015, 2, 465−469

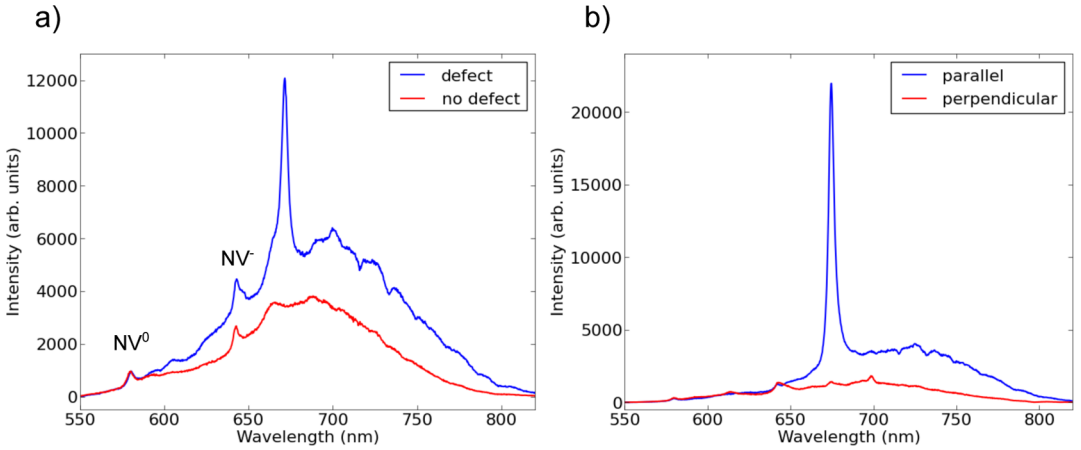

Figure 3. A cavity mode decorating the NV emission exists only in a defect cavity (a) and is shown to be linearly polarized along the axis of the defect (b). The measured Q is ∼170.

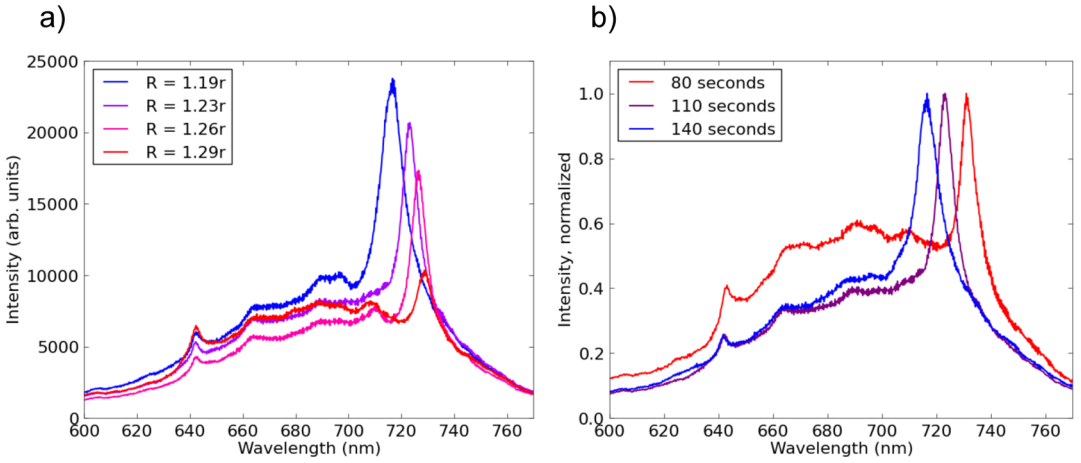

Figure 4. (a) Tuning of the cavity mode by increasing the defect size (red shift). (b) Blue-shift tuning via extended reactive ion etching to reduce the feature sizes.

Al_2O_3 onto the diamond membrane with the shallow NV layer facing up. Next, 250 nm of silver is deposited with e-beam physical vapor deposition. Next, the structure is flipped onto another Si substrate through a template-stripping process,[14,15] a technique that creates an ultrasmooth silver surface, which has previously been used for nanowire and trench-type cavities.[16−18] Finally, the diamond membrane atop the Ag−Al_2O_3 structure is thinned to a thickness between 200 and 500 nm. This template-stripping method ensures intimate contact between the diamond membrane and the Al_2O_3 layer and an atomically smooth silver surface (RMS roughness: 1−2 nm; see the Supporting Information) to support the propagation of surface plasmon modes.

The second principal fabrication challenge lies in shaping the diamond into isolated nanopillars. A photonic crystal mask is patterned onto the diamond with e-beam lithography (EBL), then transferred onto the diamond using reactive ion etching (RIE) in O_2 plasma. Underetching the diamond leads to residual diamond material that links the nanopillars at the base, which prevents confinement of the cavity mode within the defect. Overetching through the diamond and Al_2O_3 results in oxidation of the underlying silver layer and dramatically changes its optical properties, preventing the formation of plasmonic gap modes. The 5 nm of Al_2O_3 has limited capability to serve as an etch stop layer. However, using a much thicker alumina layer (>10 nm) reduces the cavity field strength at the location of the NVs. Thus, transferring the photonic crystal pattern to the diamond requires both an accurate measurement of the starting diamond membrane thickness and a careful calibration of the diamond etch rate in the reactive ion etcher (see Supporting Information for more details). This ensures that the diamond membrane is etched through to create isolated pillars, yet a sufficient thickness of the alumina layer remains to prevent the oxidation of the silver layer underneath.

Optical characterization was performed using a home-built confocal microscope with 532 nm laser excitation. A bright photoluminescence signal with peaks at 575 and 637 nm was observed in a defect-free photonic crystal. The peaks correspond to nitrogen vacancy centers in neutral and negative charge states, respectively. When the defect cavity was illuminated, we observed a clear peak from the NV phonon sideband (Figure 3a). From FDTD simulations, we expected the mode to be linearly polarized parallel to the direction of the major axis of the defect. Hence, the unpolarized background fluorescence from NVs not coupled to the cavity can be removed with a linear polarizer filter placed before the spectrometer and aligned parallel to the defect axis (Figure 3b). Rotating the polarizer filter by 90° results in minimal collection of emission from the cavity mode (Figure 3b). The highest measured Q of the cavities was ∼170, which is

DOI: 10.1021/ph500469e
ACS Photonics 2015, 2, 465−469

comparable to the simulated Q of ∼200. This is, to the best of the authors' knowledge, the highest Q measured in a diamond plasmonic photonic crystal cavity.

The measured mode in Figure 3 appears at 670 nm, red-shifted with respect to the expected 636 nm from simulations. We attribute this difference to the challenges and inaccuracies in the fabrication. Precise control of the cavity dimensions is required both in the z-direction (height of the diamond pillars) and in the lateral directions. Since the height of the diamond pillars is determined by thinning the diamond membrane via RIE, nonuniformities in the initial membrane thickness and the constraint of preventing overetching during pattern transfer limit the precision of the pillar heights. In addition, there were substantial proximity effects, despite software corrections, during EBL of the dense array of pillars for the photonic crystal pattern. The use of negative tone resist (hydrogen silsesquioxane) in lithography led to larger than anticipated feature sizes, which contributed to the red-shifted modes in the fabricated structures. We believe that these fabrication issues can be addressed in future work, and that the tuning of the mode (described below) can also compensate for the fabrication errors. Tuning the mode resonance frequency to the NV^- zero-phonon transition is an important first step toward observing resonant emission enhancement. In our design, the mode resonance frequency can be tuned by adjusting the geometry of the defect cavity, through scaling the photonic crystal lattice constant, rod radii, and defect size and configuration. As mentioned earlier, a set of cavities with different values for R and r_t were fabricated, and the corresponding mode frequencies were measured. In Figure 4a, the cavity mode shifts from 711 to 724 nm as the defect size, R, increases from 1.2r (100 nm) to 1.3r (109 nm). The 13 nm shift in the mode resonance agrees with FDTD simulations (using the measured dimensions of the fabricated cavities) where the corresponding resonance wavelengths are 739 and 751 nm, respectively. Post-fabrication, the cavity mode may also be reversibly tuned through the controlled injection and adsorption of a gas onto the cavity.[7] In addition, irreversible tuning can be accomplished by depositing thin layers of oxide on the device via ALD[16] (red shift) or by etching the diamond and reducing the rod and cavity size (blue shift). The latter process produced the tuning shown in Figure 4b. We used RIE in oxygen to reduce the size of the diamond pillars with a lateral etch rate of 3 nm/min (estimated from simulation results for the mode resonance for scaled structures). However, Q of the cavity mode decreased after etching for more than 2 min. We believe that this is due to etching through the thin Al_2O_3 layer and damaging the Ag layer underneath. Any roughening of the Ag substrate leads to higher losses as the substrate fails to sustain surface plasmon modes.

Preliminary lifetime measurements carried out did not show Purcell enhancement, likely because only a fraction of the ensemble of NVs was located at the correct depth to couple efficiently to the cavity mode. This is because the diamond samples used to fabricate the devices in these initial experiments were implanted with a high density of nitrogen, resulting in a large variation in NV depth. More accurate lifetime measurements should be made at cryogenic temperatures with a diamond sample having lower NV density, where the NV emission lifetime can be compared before and after tuning the mode into resonance with the NV^- zero-phonon transition. These considerations will also be addressed in future work for the fabrication and characterization of new cavities.

CONCLUSIONS

In summary, we have demonstrated a hybrid plasmonic photonic crystal cavity structure designed to selectively enhance near-surface emitters in diamond. Fabricated devices exhibit values of $Q \approx 170$ with a mode volume of ∼0.1 $(\lambda/n)^3$. This hybrid cavity allows coupling to near-surface NVs and affords greater flexibility in controlling the out-coupling of the emission. We have also demonstrated methods for tuning the cavity mode resonance that may be used for emission enhancement of the zero-phonon transition of NVs or silicon vacancy centers in diamond. We plan to fabricate devices using diamond samples with a lower NV density and better depth confinement with the aim of demonstrating Purcell enhancement of the zero-phonon transition of shallow-implanted NVs.

ASSOCIATED CONTENT

Supporting Information

This material is available free of charge via the Internet at http://pubs.acs.org.

AUTHOR INFORMATION

Corresponding Author

*E-mail: ehu@seas.harvard.edu.

Present Address

[⊥]HRL Laboratories, LLC, Malibu, California 90265, United States.

Notes

The authors declare no competing financial interest.

ACKNOWLEDGMENTS

The authors acknowledge the financial support of DARPA's Quantum Assisted Sensing and Read-out and AFOSR's Quantum Memories in Photonic-Atomic-Solid-State Systems programs. X.Z. and S.C. acknowledge support from the National Science Foundation through the STC Center for Integrated Quantum Materials (NSF grant DMR-1231319) and Graduate Research Fellowship Program, respectively. We also thank Dr. Kasey Russell for helpful discussions and experimental help.

REFERENCES

(1) Rondin, L.; Tetienne, J.-P.; Hingant, T.; Roch, J.-F.; Maletinsky, P.; Jacques, V. Magnetometry with Nitrogen-Vacancy Defects in Diamond. *Rep. Prog. Phys.* **2014**, *77*, 056503.

(2) Schirhagl, R.; Chang, K.; Loretz, M.; Degen, C. L. Nitrogen-Vacancy Centers in Diamond: Nanoscale Sensors for Physics and Biology. *Annu. Rev. Phys. Chem.* **2014**, *65*, 83−105.

(3) Dutt, M. V. G.; Childress, L.; Jiang, L.; Togan, E.; Maze, J.; Jelezko, F.; Zibrov, A. S.; Hemmer, P. R.; Lukin, M. D. Quantum Register Based on Individual Electronic and Nuclear Spin Qubits in Diamond. *Science* **2007**, *316*, 1312−1316.

(4) Aharonovich, I.; Neu, E. Diamond Nanophotonics. *Adv. Opt. Mater.* **2014**, 1−18.

(5) Faraon, A.; Santori, C.; Huang, Z.; Acosta, V. M.; Beausoleil, R. G. Coupling of Nitrogen-Vacancy Centers to Photonic Crystal Cavities in Monocrystalline Diamond. *Phys. Rev. Lett.* **2012**, *109*, 033604.

(6) Hausmann, B. J. M.; Shields, B. J.; Quan, Q.; Chu, Y.; De Leon, N. P.; Evans, R.; Burek, M. J.; Zibrov, A. S.; Markham, M.; Twitchen, D. J.; et al. Coupling of NV Centers to Photonic Crystal Nanobeams in Diamond. *Nano Lett.* **2013**, *13*, 5791−5796.

(7) Lee, J. C.; Bracher, D. O.; Cui, S.; Ohno, K.; McLellan, C. A.; Zhang, X.; Andrich, P.; Aleman, B.; Russell, K. J.; Magyar, A. P.; et al.

DOI: 10.1021/ph500469e
ACS Photonics 2015, 2, 465−469

Deterministic Coupling of Delta-Doped NV Centers to a Nanobeam Photonic Crystal Cavity. *Appl. Phys. Lett.* **2014**, *105*, 261101.
(8) Schietinger, S.; Barth, M.; Aichele, T.; Benson, O. Plasmon-Enhanced Single Photon Emission from a Nanoassembled Metal-Diamond Hybrid Structure at Room Temperature. *Nano Lett.* **2009**, *9*, 1694−1698.
(9) Kumar, S.; Huck, A.; Andersen, U. L. Efficient Coupling of a Single Diamond Color Center to Propagating Plasmonic Gap Modes. *Nano Lett.* **2013**, *13*, 1221−1225.
(10) De Leon, N. P.; Shields, B. J.; Yu, C. L.; Englund, D. E.; Akimov, A. V.; Lukin, M. D.; Park, H. Tailoring Light-Matter Interaction with a Nanoscale Plasmon Resonator. *Phys. Rev. Lett.* **2012**, *108*, 226803.
(11) Liu, T.; Russell, K. J.; Cui, S.; Hu, E. L. Two-Dimensional Hybrid Photonic/Plasmonic Crystal Cavities. *Opt. Express* **2014**, *22*, 8219.
(12) Bulu, I.; Babinec, T.; Hausmann, B.; Choy, J. T.; Loncar, M. Plasmonic Resonators for Enhanced Diamond NV-Center Single Photon Sources. *Opt. Express* **2011**, *19*, 5268−5276.
(13) Magyar, A. P.; Lee, J. C.; Limarga, A. M.; Aharonovich, I.; Rol, F.; Clarke, D. R.; Huang, M.; Hu, E. L. Fabrication of Thin, Luminescent, Single-Crystal Diamond Membranes. *Appl. Phys. Lett.* **2011**, *99*, 081913.
(14) Nagpal, P.; Lindquist, N. C.; Oh, S.-H.; Norris, D. J. Ultrasmooth Patterned Metals for Plasmonics and Metamaterials. *Science* **2009**, *325*, 594−597.
(15) Hyuk Park, J.; Nagpal, P.; Oh, S. H.; Norris, D. J. Improved Dielectric Functions in Metallic Films Obtained via Template Stripping. *Appl. Phys. Lett.* **2012**, *100*, 081105.
(16) Russell, K. J.; Liu, T.-L.; Cui, S.; Hu, E. L. Large Spontaneous Emission Enhancement in Plasmonic Nanocavities. *Nat. Photonics* **2012**, *6*, 459−462.
(17) Liu, T.; Russell, K. J.; Cui, S.; Hu, E. L. Controlled Mode Tuning in 1-D "RIM" Plasmonic Crystal Trench Cavities Probed with Coupled Optical Emitters. *Opt. Express* **2013**, *21*, 30074−30081.
(18) Vesseur, E. J. R.; Polman, A. Controlled Spontaneous Emission in Plasmonic Whispering Gallery Antennas. *Appl. Phys. Lett.* **2011**, *99*, 231112.

DOI: 10.1021/ph500469e
ACS Photonics 2015, 2, 465−469